Plant Physiol. (1985) 79, 41–56
0032-0889/85/79/0041/16/$01.00/0

A Novel Method of Natural Cryoprotection[1]

INTRACELLULAR GLASS FORMATION IN DEEPLY FROZEN *POPULUS*

Received for publication November 20, 1984 and in revised form March 28, 1985

ALLEN G. HIRSH*, ROBERT J. WILLIAMS, AND HAROLD T. MERYMAN
American Red Cross, Biomedical Research Laboratories, Bethesda, Maryland 20814

ABSTRACT

Correlating measurements from differential scanning calorimetry, freeze-fracture freeze-etch electron microscopy, and survival of twigs after two-step cooling experiments, we provide strong evidence that winter-hardened *Populus balsamifera* v. *virginiana* (Sarg.) resists the stresses of freezing below −28°C by amorphous solidification (glass formation) of most of its intracellular contents during slow cooling (≤5°C per hour). It is shown that other components of the intracellular medium go through glass transitions during slow cooling at about −45°C and below −70°C. This 'three glass' model was then used to predict the results of differential scanning calorimetry, freeze-fracture freeze-etch electron microscopy, and biological experiments. This model is the first definitive explanation for the resistance of a woody plant to liquid N_2 temperatures even if quench cooling (1200°C per minute) begins at temperatures as high as −20°C and warming is very slow (≤5°C per hour). It is also the first time high temperature natural intracellular glass formation has been demonstrated.

A small group of woody plants native to the subarctic regions of the northern hemisphere has been shown to possess resistance to temperatures near absolute zero (4, 16). Gradations of this complete cold hardiness can be characterized by the term 'quench-hardiness'. This concept of quench-hardiness is derived from work by Sakai and Otsuka (9–12) in the 1960's. They showed that even after woody tissue became resistant to exposure to LN_2[2] (−196°C) during fall hardening, further hardening was demonstrable. They noted a continued increase in the maximum temperature from which quench cooling of the tissue in LN_2 (cooling rates >1200°C/min) could commence after initial slow cooling (<5°C/h) and still yield viable tissue upon thawing. This maximum temperature is designated here as T_q. They warmed the tissue at 1 or 2°C/min or faster and used ability to plasmolyze and deplasmolyze immediately after thawing as a viability assay. Unfortunately, these fast warming rates can allow a tissue to escape damage from nonequilibrium freezing events in the intracellular fluids, and the viability assays must be carried out for several weeks to give reliable results (4). Thus, Sakai's results suggest that a completely hardy plant's osmotically concentrated intracellular fluids can increase their ability to resist ice formation beyond that necessary to avoid ice formation at ambient rates of cooling to extreme subzero temperatures, but these results were not definitive.

Sakai went on to postulate that completely hardy cells died when the quenching temperature was too high because very small, noninjurious ice crystals which were formed during fast cooling recrystallized to larger, injurious crystals upon warming. As proof of this assertion, he offered photographs of fixed and sectioned specimens examined in the electron microscope (11), which showed gaps interpreted as the result of intracellular ice formation. We have re-examined the nature of complete hardiness using more careful criteria of viability and the physical measurement methods of DSC and freeze-etch EM using the local poplar species, *Populus balsamifera* var. *virginiana* (Sargent). We had three alternative models in mind. Completely hardy cells: (a) are capable of withstanding considerable intracellular freezing; (b) withstand massive dehydration during deep freezing such that at low temperatures all remaining water is water of hydration (bound water); or (c) form aqueous glasses intracellularly during freezing to low temperatures, glasses which remain amorphous solids at relatively high subzero temperatures. We will demonstrate here that, in *P. balsamifera*, model (c) is the most appropriate.

MATERIALS AND METHODS

Biological. Hardy twigs were harvested and used either fresh, stored at +4°C on moist perlite, or stored at −20°C with ice in a mechanical freezer until ready for use. Experiments were always accompanied by a control. Experiments usually involved two groups of twigs in large-capped polyethylene centrifuge tubes (6/tube) placed into a cold alcohol bath (LT-50 or ULT-80, Neslab Company, Needham, MA) and cooled to the appropriate temperature (T*) at 3°C/h (subsequently referred to as slow freezing). The experimental group was then plunged into LN_2 with the caps removed from the tubes so that the liquid was in direct contact with the twigs, or, if it was plunged into dry ice, the twigs were buried in dry ice. In LN_2, boiling ceased in less than 10 s so that the cooling rate was in excess of 1,200°C/min. This rate was verified by inserting thermocouples into the cortex of the twigs and measuring the cooling rate with a digital thermometer (BAT-12, Bailey Instruments, Saddlebrook, NJ; 0.5-s response time). It was found to be 1200°C/min from −20°C to −144°C. The twigs so quenched were then either: (a) immediately reinserted into the cold alcohol bath at T* for fast rewarming to the bath temperature (about 10°C/min as measured by thermocouples in the twigs); (b) stored in dry ice or LN_2, then reinserted after the bath had been warmed to a higher temperature at 3°C/h; or (c) stored in dry ice or LN_2, then reinserted after the bath had been cooled at 3°C/h to some lower temperature. The control samples remained in the bath throughout. Thus, most comparisons were between slowly frozen and quickly frozen samples.

[1] Supported in part by National Institutes of Health grants BRSG 2 SO7 RR 05737 and GM 17959 and a grant from the Nerkin Foundation. Contribution No. 649 from the American Red Cross Biomedical Research Laboratory. This work taken in part from the Ph.D. Thesis of Allen G. Hirsh, Department of Horticulture, University of Maryland, College Park, MD.

[2] Abbreviations: LN_2, liquid nitrogen; DSC, differential scanning calorimetry.

For maximally quench-hardy *Populus*, slow freezing to −70°C and subsequent slow warming (3°C/h) results in almost zero mortality and it appeared unnecessary to have an additional unfrozen control. After reinsertion in the bath, both the control and experimental groups of twigs were slowly warmed until thawed (or occasionally warmed as fast as the bath would go; at 0.5 to 1°C/min) and thereupon placed in wet Perlite (Schundler Co., Metuchen, NJ) in beakers covered with Parafilm (Dixie-Marathon, Greenwich, CT) and stored for no less than 2 d at +4°C before being moved to a well-lit shelf at room temperature. Mortality and growth were monitored for 3 to 5 weeks by observation under a dissection microscope and by plasmolysis-deplasmolysis in $CaCl_2$ solutions under a light microscope. The latter was often recorded on videotape. Twigs were considered alive if after 3 weeks they remained essentially free of disease, showed healthy green cambium, had the cellular characteristics of spring twigs (dispersed chloroplasts, low osmolality) and could successfully plasmolyze and deplasmolyze twice in 5% $CaCl_2$ (1.25 osm). Also, the maturation of buds and/or callosing (growth of undifferentiated tissue) was monitored during this period. The callose could be easily distinguished at X 50 in the dissection microscope by the gradual appearance over a period of several days of large amorphous cell masses protruding from the cut end or sides of the twigs. Statistical tests were performed on these callusing/bud break data as well as on the total mortality data.

Since pairwise statistical comparisons were used, an exact probability test based on the Polya Urn model was devised. The latter refers to the probability of picking n live (or callosing/bud breaking) twigs and m dead (or nongrowing) twigs out of a container containing $A>n$ live (or callosing/bud breaking) twigs and $B>m$ dead (or nongrowing) twigs if the picking is done without replacement. The null hypothesis was that both experimental and control observations came from the same group with total mortality (or regrowth potential) equal to that of experimental plus control. A computer program was written calculating the probability of choosing the observed experimental group from such a larger group plus the probability of choosing all less likely groups. The test is thus two-tailed.

The equation for the probability (P) of choosing a particular set of n,m is:

$$P = \frac{(n+m)!\ A!\ B!\ ((A+B)-(n+m))!}{n!\ m!\ (B-m)!\ (A-n)!\ (A+B)!}$$

Differential Scanning Calorimetry. *Theory.* Differential scanning calorimetry is a technique, developed originally at the Perkin Elmer Corporation of Norwalk, CT, for measuring the power necessary to keep an experimental sample isothermal with a reference sample when both samples are being heated or cooled at a constant rate. Figure 1 is a schematic (from Perkin Elmer) of the measuring apparatus. The heavily outlined figure is the sample pan holder, labeled (A), a platinum cup. The rectangular regions, labeled (B), containing the symbols R_s and T_s on the left, and T_r on the right represent the sample pans. These are aluminum sample holders, one type of which can be sealed against up to 3 atmospheres of pressure by simply crimping an aluminum top over it. Thus, accurate measurements can be made on volatile materials. The region labeled R_o is the region of contact between the sample pan and the sample pan holder. Usually, this is largely a thin air space (the area of actual metal to metal contact is small because the bottoms of the sample pans are not perfectly flat). Immediately below this region, in the area labeled T_p, are highly accurate platinum resistance thermometers (C), and the resistance heaters, (D). Both of these are located just beneath the floor of the platinum sample pan holder. The large rectangle enclosing the two cups represents a large aluminum heat sink. This is held at LN_2 temperature during studies conducted at temperatures below 0°C. The Rs represent various thermal resistances (unit = degrees/unit power). Thus, R is the resistance of the heat conduction path from the platinum cup to the heat sink, R_e the source resistance of the electronic circuits, R_o the resistance from the sample pan to the temperature sensor, and R_s the internal resistance of the sample.

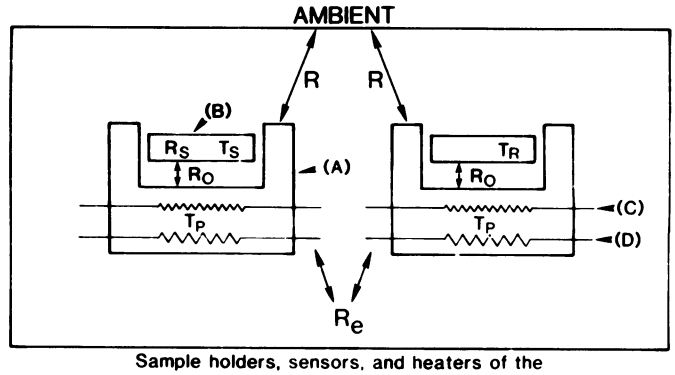

FIG. 1. Schematic of differential scanning calorimeter. (A), Platinum sample holding cup; (B), Aluminum sample pan; (C), Pt resistance thermometer (sensor); (D), ohmic heating element; (R), thermal resistance of holding cup to surround; (R_s), internal thermal resistance of sample; (R_o), thermal resistance of sample pan-holding cup contact; (T_p), temperature of sensor; (T_r), temperature of reference sample; (T_s), temperature of experimental sample. Figure reproduced with permission of Perkin Elmer Corp., Norwalk, CT.

The system maintains isothermality between sample and reference by reading the average voltage of the two sensors 60 times/s and comparing each reading to a reference voltage determined by a clock in the microprocessor unit of the DSC. The clock varies the reference voltage between the starting and final voltages of each scan so as to provide a linear ramp of temperature at a rate set by the experimenter. Alternating with these adjustments of the average voltage of both samples to the reference voltage of the temperature ramp, the difference in voltage between the sensors is fed into an amplifier and current is supplied to both heater circuits so as to minimize the difference in voltage between the sensors. Since the resistance of the heater is known to great accuracy, by Ohm's law the differential power between sample and reference necessary to maintain isothermality can be determined directly from the differential current.

The differential current readings, which are proportional to the differential heat flow between sample and control, are fed through an electronic signal processing unit that averages approximately 30 readings at a time, and this average is in turn fed to a microcomputer. These averages are then displayed on a power *versus* temperature graph on a video screen. After the scan has ended, these data can be stored permanently on a magnetic disc and manipulated by means of Perkin Elmer software (TADS Standard Software Kit, Perkin Elmer Corp., written in Basic). Further details of DSC operation may be found elsewhere (7).

Preparation of Samples. Aliquots of experimental material or of substances with known thermal behavior such as aqueous $CaCl_2$ or aqueous PVP were placed in sealable aluminum sample pans and sealed with a crimper press. The sealed sample pan was then weighed to 10 μg on a Cahn Electrobalance (Model G, Cahn Instrument Co., Paramount, CA). After weighing, the sample pans were transferred to the platinum sample holders of the DSC-4 at a temperature controlled by the DSC microprocessor and microcomputer. Despite the fact that water poses theoretical problems as a temperature and enthalpy standard, the fact that all of our samples were aqueous solutions convinced us to use double-distilled H_2O as our standard. If the samples used

were dilute polymer solutions and it was desired to measure highly concentrated solutions, an aliquot of dilute solution was loaded in an open sample pan and allowed to evaporate water until the weight of remaining sample indicated that the proper concentration had been attained. The samples were then rapidly sealed and reweighed. If the samples were unfrozen wood, adhering water was blotted dry before sealing and weighing.

Samples of frozen (stored) wood were treated in two different ways. If it was desired to measure in a sealed sample pan, the wood was fractured in dry ice environment and loaded in a sealable pan in the dry ice environment taking care to exclude dry ice from the pan. Then the top of the pan was put in place and the pan transferred to the precooled base of the crimper. Dry ice was then piled over the covered pan and crimper base so that the sealing plunger would contact the sample lid by passing through dry ice. Thus, warming of the sample was minimized. If it was desired to measure large samples of wood, larger, unsealable aluminum pans were used. These were loaded in a dry ice environment and unsealed aluminum covers were placed over the wood samples. The samples were subsequently held in the DSC at −50°C for at least 10 min to drive off traces of dry ice. All sample pans containing frozen wood were transferred to the DSC-4 sample pan holders in blocks of dry ice. If samples were initially frozen, they were generally weighed quickly after thawing at the end of an experimental sequence.

Freeze-Fracture Freeze-Etch Electron Microscopy. Samples were prepared in several different ways for freeze-fracture freeze-etch studies. Ordinarily, vascular plant tissue is cut into small parallelopipeds approximately 1 × 0.5 × 0.5 mm and inserted into gold holders such that the plane of fracturing is perpendicular to the long axis of the fibers. We used the holders many times but there was a severe problem associated with them when wood was used as the tissue. The deeply frozen wood often did not crack but simply carried the ice that it was imbedded in with it so that the whole sample remained in one or the other tooth of the holder. Even if the wood did crack, as much as 90% of the time the cracked surface produced immensely distorted replicas which subsequently disintegrated during acid cleaning.

In the most successful runs, material was cracked in the open air at dry ice temperature. Large fractured surfaces of many square mm were produced in this way. Samples several mm square were then placed bark face up in a melted pool of 57% glycerol-water solution (glass transition at −110°C) and immersed in LN_2. The glycerol-water was allowed to solidify, the sample was refractured under LN_2, and etched at temperatures between −98° and −80°C. This relatively high etching temperature produced clean replicas uncontaminated by condensed volatiles of unknown composition. Samples were transferred to the freeze etch unit and held at −110°C until a good vacuum was achieved. This high holding temperature during evacuation of the replicating chamber also proved crucial in preventing condensation of contaminants.

Etching was accomplished by raising the temperature of the sample from −110°C to between −80° and −98°C and allowing any ice to sublime; the rate of sublimation increases exponentially with temperature, following the Clapeyron equation. After a period of time varying from 1 to 15 min, the temperature was dropped to −196°C and the platinum-carbon shadowing was begun. Generally, the ferocity of the usual tissue removal method using acid hydrolysis broke the replicas into such small pieces that almost all replica surface was lost.

Recently Steere and Erbe (13) have perfected a new technique that has allowed us to obtain large sheets of replica of wood routinely. Basically, the technique consists of coating the newly made replica with a 2% Lexan solution, a polycarbonate plastic dissolved in ethylene dichloride, immediately after each replica is made and allowing the ethylene dichloride to evaporate in a small freezer at about −10°C. The replica, now held together by acid-resistant plastic, is then run through the acid digestion process to remove the subtending wood.

Once replicas were cleaned in acid and washed in distilled H_2O, they were placed on small copper grids with electron-clear plastic collodion stretched over them. These were then placed in a clearing solution of ethylene dichloride to remove the Lexan (collodion is resistant to this solvent).

Replicas were examined in a JEOL JEM-100 transmission electron microscope. Photographs were made in stereo pairs, with one photograph rocked 10°C with respect to the other by use of a goniometer stage in the microscope. Photographs were imprinted on Kodak glass electron image plates and are here reproduced such that all shadows are black, as in nature. Shadows face downward to give a proper stereoscopic image.

The primary goal of the electron microscope study was to ascertain whether evidence of ice could be seen as a result of a particular freezing stress of the tissue. The criteria for claiming that ice was or was not present in the sample are the presence of clustered holes (etching) in the replicas which indicate that ice crystals have sublimed away leaving ridges of solidified glassy solution in between them. It is well established that glassy solutions show no evidence of etching *in vacuo* at temperatures below the glass transition of the solutions (2, 6, 15).

Identification of Nonequilibrium Phase Changes. Figure 2 shows the calorimetric behavior of a 77% PEG:H_2O solution. Its thermal behavior is well characterized, and illustrates the major events which allow us to assert that the intracellular solutions of the hardy *Populus* are aqueous glasses. When this PEG solution is cooled at 100°C/min to −160°C then warmed at 80°C/min to the thawed state (solid line), several prominent thermal events are recorded. The glass transition, labeled a_1, is identifiable as a glass transition by its classic S shape (1). Additionally, by repeating the 100°C/min cooling but warming more slowly (not shown), one notes that the change in specific heat capacity

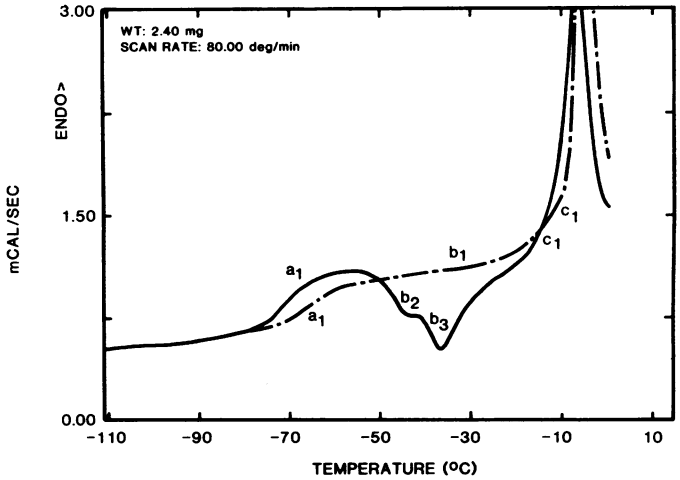

FIG. 2. A 1.0:3.3 H_2O-polyethylene glycol (PEG mol wt 8000) solution, w/w, was cooled at 100°C/min to −160°C then warmed at 5°C/min to −15°C, recooled at 100°C/min to −160°C, and finally warmed at 80°C/min to thaw as shown by the dashed line. On the dashed line, a_1 represents the glass transition, b_1 a slight devitrification, and c_1 the equilibrium melting of the ice in the system. The solid line is the 80°C/min warming of the same sample after cooling 100°C/min to −160°C from the thawed state. The a_1 transition is the glass transition. Note that it is at a lower temperature and involves a larger change of heat capacity than the recooled material. This indicates a more dilute aqueous glass. Note also the large devitrification (b_2, b_3) = b_1, also an expected result of increased water content. The melt c_1 is virtually the same as in the first run; the slight shift in the onset of melting is unexplained.

(vertical displacement of the trace) remains the same. Also, there is no initial endothermic overshoot characteristic of the temporarily infinite heat capacity of a first order phrase transition such as a eutectic melt. Additional evidence that the solution is a melted glass above about −70°C is provided by the exothermic events b_1, b_2. These represent the continued growth (devitrification) of ice from previously condensed submicroscopic ice nuclei, formed during cooling at temperatures below that which will support ice growth at an observable rate (homogeneous nucleation). Thus, it is not until the solution is warmed above the point at which ice nuclei formed during cooling that ice formation will occur at rates sufficient to produce a signal recordable on the calorimeter. The dual peak implies at least two different crystal growth domains, each with a different dependency of growth rate on temperature. The actual equilibrium melt of the ice so formed begins at c_1, about −15°C. The heating rate, 80°C/min, is much too fast for the machine to yield accurate melting temperatures for first order phrase transitions; they will appear to be at a significantly higher temperature than known values. Nevertheless, a further confirmation of the interpretation of these events is provided by integrating the area of the devitrification exotherms and comparing it to the area of the melting exotherm. That area represents the total ΔH of the transitions. The two integrations agree quite well if the change in heat of fusion of ice with temperature is taken into account. Thus, almost all the ice forms from devitrification during warming.

Based on the fact that the magnitude of the glass transition in most aqueous glasses is linearly dependent on the number of water molecules per colligative unit of solute (1), one would predict that if the water content of the glass falls then the magnitude of the change in heat capacity at the glass transition would drop. Furthermore, it is also generally observed that the lower the water content of a glass-forming solution, the higher the glass transition temperature. Thus, allowing ice to grow during devitrification of a water-polymer melt which is incapable of forming a eutectic should decrease the size of the glass transition and elevate its temperature. This is what we see in the dashed curve of Figure 2. Here, the solution was first cooled at 100°C/min to −160°C, warmed at 5°C/min to −15°C, recooled at 100°C/min to −160°C, and finally warmed as shown here at 80°C/min. The 5°C/min warming to −15°C allowed nearly complete devitrification to occur, but recooling from −15°C prevented any significant remelting to occur. The results are as predicted: the glass transition is smaller in magnitude, at a higher temperature, and followed by almost no devitrification. Thus, in examining the living wood and using the cells as osmometers by holding them at various high subzero temperatures in the presence of extracellular ice before quick cooling, we have looked for endotherms displaying the same behavior as these artificial polymer-H_2O systems.

RESULTS

Biological. Figures 3 and 4 illustrate key results of quenching experiments on hardy *Populus* with T_q >−20°C and *Populus* with T_q <−20°C; *i.e.* maximally and submaximally quench-hardy, respectively. In these experiments, twigs were cooled at 3°C/h to the desired quenching temperature (shown as the beginning of each curve on the T axis). Quick cooling (1200°C/min) was effected by immersion in LN_2. Controls either were held at the quenching temperature or were slowly frozen to temperatures at or below −50°C. All quenched samples were warmed by insertion into centrifuge tubes in a temperature bath. As can be seen, fast warming (10°C/min) was much slower than fast cooling. The mortality was complete in a sample of submaximally quench-hardy twigs (solid line Fig. 3) if quenching commenced at −20°C. It was a high 75% but not complete (and marginally distinguishable from control c's 45% mortality, P = 0.045) when

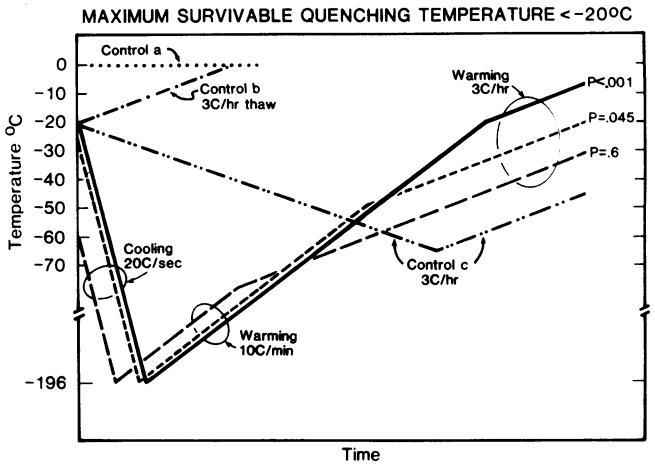

FIG. 3. Cooling regimen for submaximally quench-hardy *Populus*. The point of origin on the abscissa indicates temperature to which the tissue was frozen at 3°C/h. The lines then descend, the slope indicating qualitatively the rate of cooling in LN_2. The first section of ascending lines indicates the rate of uncontrolled warming in an alcohol bath. The break in slope in the ascending lines indicates a temperature at which controlled 3°C/h warming recommended. The material analyzed here is submaximally quench-hardy. When it was quenched from −60°C and reinserted at −80°C and then warmed slowly to thaw (long dash line), it showed no increase in mortality above control ($p = 0.6$, control *a* survival = 87%, experimental = 80%, null hypothesis = no significant difference in mortality between control and experimental samples). When the twigs were quenched from −25°C and reinserted at −50°C for slow warming (short dashed line), the difference between the experimental survival and control was barely significant ($p = 0.045$, control *c* survival = 54%, experimental = 24%), despite the fact that the time allowed for possible devitrification between −50°C and −25°C was 8 h. When the material was quenched from −20°C, then warmed so that the total elapsed time allowed for devitrification for the entire range −135° to −20°C was only 11 min (solid line), a highly significant difference in mortality was nevertheless observed ($p < 0.001$, control *b* survival = 77%, experimental = 0%), indicating that the intracellular solution became significantly less stable when quenching commenced after equilibration with ice at −20°C.

quenching was from −25°C (short dash line). Mortality in maximally quench-hardy twigs (dashed and dot-dashed lines Fig. 4) with quenching from −20°C was 23% *versus* 7% for controls (control b plunged into dry ice) with a P of 0.35 (not distinguishable). When the quenching temperature of fully quench-hardy twigs was −15°C (solid line), the difference was dramatic with mortality at 100% and P = 10^{-16}. This implies a very large change in the ice forming characteristics of the quench cooled, maximally quench-hardy intracellular medium when the equilibrium temperature of the intracellular solutions is shifted from −15° to −20°C. The probabilities reported here (in both Figs. 3 and 4) are for live twigs *versus* dead twigs.

The results clearly support a T_q slightly above −20°C for the maximally quench-hardy twigs. If differences in callosing and/or bud break after quenching in LN_2 from −20°C are compared with differences in total mortality after quenching from −20°C they are both found indistinguishable from controls and thus by both criteria the T_q is the same. Thus, no evidence was seen for a differential increase in damage after extreme freezing stress between the two criteria: cell reproduction as opposed to cell survival.

The maximally quench-hardy material displayed no difference in mortality when 10°C/min warming continued from −196°C to the original quenching temperature as opposed to slow warming (3°C/h) after reinsertion at a much lower temperature such as −70°C. This is illustrated by the P = 0.81 and P = 0.35 curves

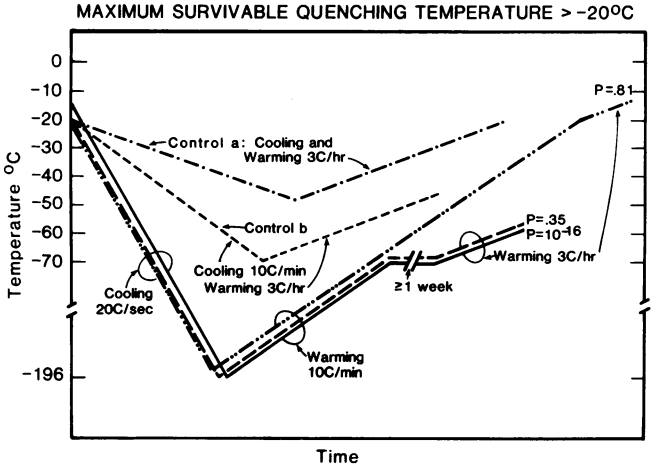

FIG. 4. Cooling regimen for maximally quench-hardy *Populus*. The point from which descending curves begin on the abscissa indicates the quenching temperature, the temperature at which quick cooling began after cooling at 3°C/h. In this case, the dash and double dot-dash curves show material quenched in LN_2 from −20°C while the solid curve shows material quenched from −15°C. The material quenched from −15°C was warmed at 10°C/min to −70°C, stored at that temperature 1 week, then thawed at 3°C/h. Mortality was complete and highly significant ($p = 10^{-16}$, control *a* survival = 95%, experimental = 0%). Material quenched from −20°C but otherwise treated identically (dashed curve) showed no significant increase in mortality over control ($p = 0.35$, control *b* survival = 92%, experimental = 76%). Material quenched from −20°C and warmed relatively rapidly back to −20°C also showed no significant damage ($p = 0.81$, control *a* survival = 69%, experimental = 65%). Thus, the instability to devitrification of the intracellular glassy melt begins when the melt composition is in equilibrium with ice at between −15° and −20°C.

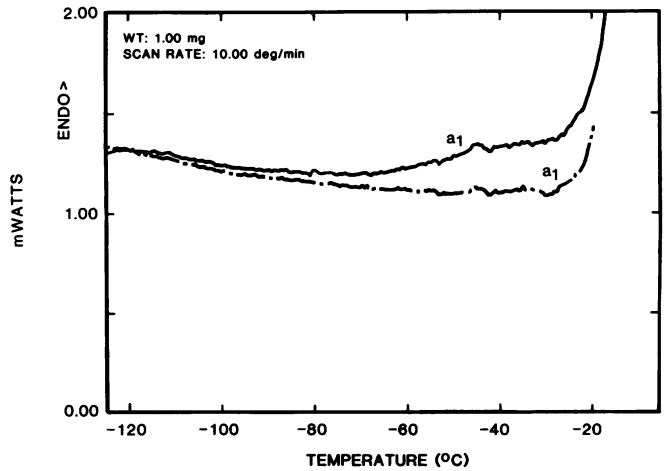

FIG. 5. Slow warming of a maximally quench-hardy sample of about 10 mg (the exact weight was not recorded; default weight of 1.00 mg). The dashed line represents 10°C/min warming after 3°C/h cooling to −70°C. Note the sudden jump into melting behavior at a_1, indicative of an equilibrium glass transition. The solid line represents 10°C/min warming after 10 min annealing at −20°C and 100°C/min recooling to −160°C. Note the great increase in magnitude and drop in the temperature of onset of event (a_1). Note also that the glass transition is not followed by a devitrification exotherm, indicating all microdomains were stabilized against homogeneous nucleation by the time the solution had equilibrated with ice at −20°C.

(quench from −20°C) of Figure 4. Thus, there was no evidence that warming rate effects recovery after quench cooling from T_q.

In an experiment not illustrated, 24 maximally quench-hardy twigs were cooled at 3°C/h to −20°C, quench cooled at 1200°C/min in LN_2, reinserted in a −27°C temperature bath (10°C/min warming), held at −27°C for 12 h, recooled at 1°C/min to −70°C, then warmed to that at 3°C/h. Survival was 70% *versus* 85% (P = 0.49) for controls just frozen to −20°C and thawed at 3°C/h. Thus, though given 12 h to produce intracellular ice at −27°C, maximally quench-hardy cells quenched from −20°C showed no increase in mortality over controls. Cells in active summer growth were not examined as they exhibit 100% mortality after freezing to −2°C.

Differential Scanning Calorimetry. Figure 5 shows a 10°C/min warm (dashed curve) of a maximally quench-hardy *Populus* sample which had been cooled to −70°C at 3°C/h, then stored at that temperature for several months. Note the sudden endothermic jump into equilibrium melting at a_1 (about −28°C). This is characteristic of aqueous solutions whose glass transition is the same as the equilibrium melting point of ice in those solutions. We term these, 'equilibrium glasses.' The solid curve is the warming of the same sample after it had been annealed 10 min at −20°C followed by cooling at 100°C/min to −160°C. The biological results demonstrate that fast cooling from −20°C is not lethal even if followed by very slow warming. The solid curve shows why this is so. The composition of the intracellular solution in equilibrium at −20°C has a higher water content than it would have if it had been in equilibrium at −28°C. As a result, the glass transition would be expected to occur at a lower temperature and have a larger amplitude. Thus, event a_1, on the solid curve is a glass melt and its change of position and amplitude are as predicted. There is no evidence of devitrification at temperatures above the glass melt on the solid curve. Thus, this solution forms a stable glass at this heating rate. Most probably it had no ice nuclei in it from homogeneous nucleation or, a less likely possibility, resisted the growth of the few intracellular ice nuclei that may have been present. The lack of devitrification is consistent with the high survival upon quenching from −20°C because it shows that, despite a significant lowering of the glass transition temperature to <−40°C from the apparent equilibrium value of −28°C, the intracellular solution in equilibrium at −20°C remains resistant to ice formation on warming from temperatures as low as −160°C.

Figure 6 shows the warming of the same sample as Figure 5 after annealing for 10 min at −10°C followed by cooling at 100°C/min to −160°C (solid curve). The dashed curve is the same as the dashed curve in Figure 5 (warming immediately after removal from storage at −70°C). Note that the glass transition a_1 has moved from the region between −70° and −40°C seen in the −20°C annealed material (solid curve, Fig. 5) to between −90° and −55°C on this solid curve. These results are an expected consequence of the increased water content of the material in equilibrium at −10°C. Longer annealing times produced no change in curve configuration so 10 min was enough time to achieve virtual intracellular equilibration with extracellular ice. In this run, annealed at −10°C, there is also a devitrification event, b_1. This is an expected consequence of the formation of observable intracellular ice on warming, as illustrated directly by the electron microscope results and the 100% mortality shown by twigs quenched from temperatures >−15°C (see biological and electron microscope results).

Figure 7 shows the warming of the same sample as in Figures 5 and 6 after it was re-equilibrated at −5°C, cooled at 100°C/min to −20°C, annealed 10 min at −20°C, then cooled at 100°C/min to −160°C (solid curve). Light microscope examination of plasmolysis-deplasmolysis cycles of thawed maximally quench-hardy cells previously quenched into LN_2 from lethally high

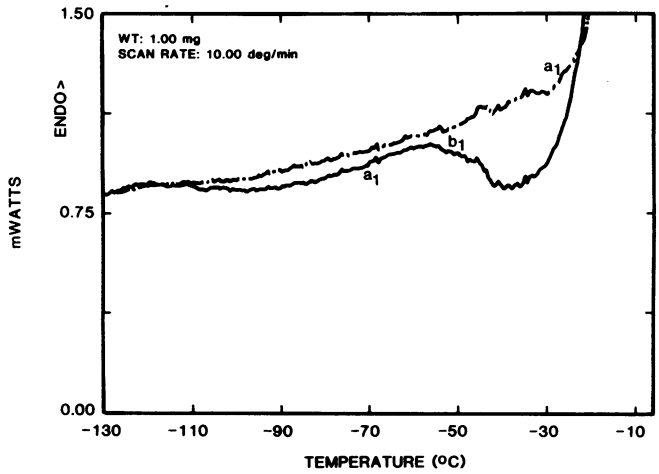

FIG. 6. Same sample as Figure 5. Again, the dashed line is 10°C warming after cooling at 3°C/h to −70°C. The solid line is 10°C/min warming after annealing 10 min at −10°C then 100°C/min cooling to −160°C. Note that a_1 on the solid line is even larger than a_1 on the solid line representing warming of the sample after annealing at −20°C (Fig. 5). The event a_1 on this solid line has also shifted to an even lower temperature than after −20°C annealing. Here, however, the glassy melt devitrifies as shown by event b_1, at about −60°C. Thus, the intracellular solution, fast cooled from equilibrium at −10°C, is unstable to ice growth upon warming.

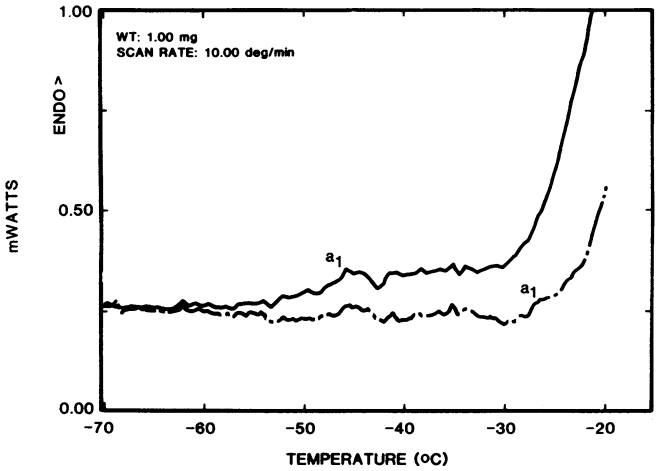

FIG. 7. If the cellular system is acting as a nearly perfect osmometer at temperatures greater than −28°C, then reannealing the sample initially equilibrated at a high temperature at a lower temperature but still above −28°C, should restore the thermal characteristics of equilibrium at the lower temperature. Shown is the 10°C/min warming of the sample after 100°C/min cooling from −5°C to −20°C then 10-min annealing at that temperature followed by 100°C/min cooling to −160°C. Note that once again only stable glass transitions a_1 are seen, no devitrifications are seen. Not only does this fit the three glass model, but also shows that, despite lethal intracellular freezing (Fig. 6), there is no immediate loss of: (a) the ability of the cells to act as osmometers; (b) the ability of the plasmalemma to resist penetration by extracellular ice; and (c) the ability of the cells to avoid heterogenously nucleating intracellular ice during deep supercooling. Since all of the cells were lethally injured, this degree of intactness is remarkable.

subzero temperatures shows that up to 10 d must pass before significant loss of membrane semipermeability in $CaCl_2$ solutions is evident. Thus, despite lethal injury, one would expect that reannealing of the sample at −20°C would return the system to the same behavior as displayed in Figure 5. This is indeed seen. The glass transition a_1 has returned to the −70°C to −40°C interval and all evidence of devitrification is absent. Thus, the amount of intracellular freezing caused by quenching from −10°C followed by slow rewarming appears insufficient to immediately destroy the osmometric behavior of the cells or induce a significant increase in intracellular heterogeneous nucleation sites.

The 10°C/min warming curves illustrate the behavior of the primary intracellular glass forming constituent(s). More subtle transitions cannot be distinguished from noise. Since the signal size for glass transitions increases roughly linearly as a function of increased warming rate, warming studies were conducted at 50°C/min as well as 10°C/min. At the higher scan rates, the temperature at which a transition occurs is less accurately measured.

Figure 8 shows the warming curves of a submaximally quench-hardy sample (maximum survivable quenching temperature about −30°C). The twigs from which this sample was taken had originally been cooled at 3°C/h to −20°C then at 1°C/min to storage at −70°C. Comparison with the DSC records of the warming of maximally quench-hardy material equilibrated at −20°C (Fig. 6) indicates that in the submaximally quench-hardy samples, some further loss of intracellular H_2O to extracellular ice must have occurred during cooling and storage, *i.e.* at temperatures below −20°C, until all of the intracellular contents had a glass transition at or above −70°C. In other words, the comparison indicates that the initial intracellular equilibrium value in the stored material was probably below −20°C. The solid curve shows the sample immediately after removal from storage at −70°C. Event a_1 is the glass transition and b_1 appears to be a small devitrification. Since this tissue survived slow warming from −70°C, event b_1 on the solid curve does not represent a lethal amount of intracellular freezing at the whole tissue level, though some cells may have been killed. The dashed curve

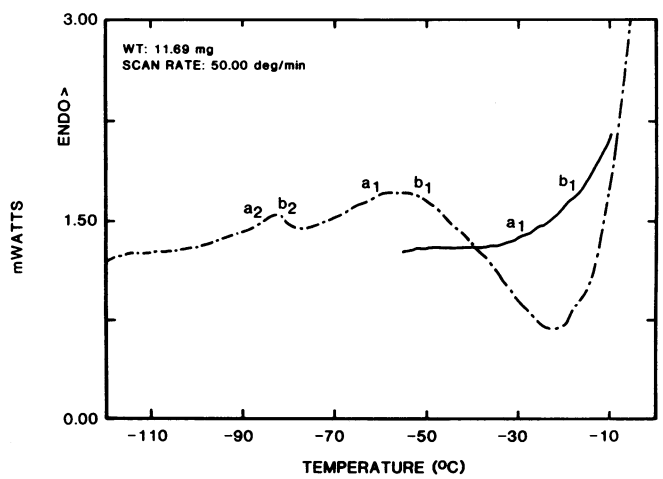

FIG. 8. First of a series of figures showing a submaximally quench-hardy sample that was initially cooled slowly to −20°C, plunged into dry ice, and stored at that temperature for several months. The solid curve in this graph shows the first 50°C/min warm of the sample (after 10 min annealing at −30°C to sublime dry ice). Note a complex glass transition at a_1 and a slight devitrification at b_1. Since the twigs from which this sample was derived subsequently survived slow warming from −70°C, b_1 on the solid curve could not be a lethal event in a significant number of cells. This curve contrasts with the dashed curve which shows the warming of the same sample after 10-min annealing at −5°C followed by 100°C/min cooling to −160°C. Events equivalent to those on the solid curve are so labeled. Note that a_1 is much larger as is the devitrification b_1 and both occur at a much lower temperature. Note that another glass transition-devitrification a_2, b_2 is now evident at about −80°C.

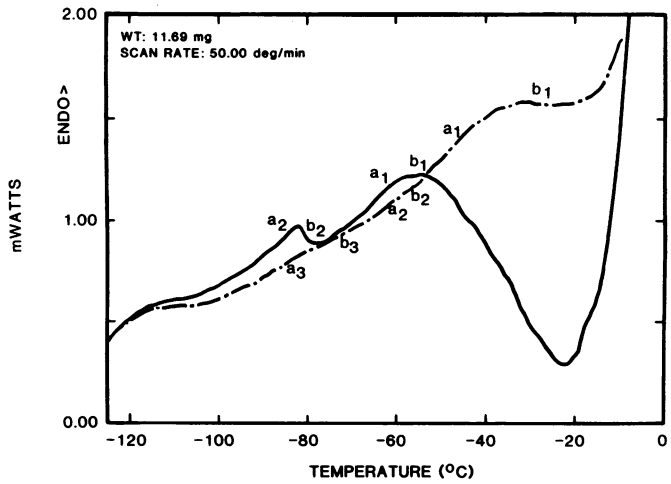

FIG. 9. Same submaximally quench-hardy sample as in Figure 8. The solid curve represents the 50°C/min warming of the sample after 10-min annealing at −5°C followed by 100°C/min cooling to −160°C. The dashed curve shows the 50°C/min warming of the sample after 3 min annealing at −10°C followed by 100°C/min cooling to −160°C. This is an insufficient time for the cells to equilibrate with extracellular ice. As a consequence, the intracellular contents were in equilibrium with ice at a temperature between −10° and −20°C. The major high-temperature glass transition-devitrifications are at a_1, b_1 on both curves. Note that it is at lower temperature and larger on the solid curve, as expected, but is considerably larger on the dashed curve than the transitions of the −70°C stored wood, in equilibrium at between −20° and −28°C shown on the solid curve of Figure 8. The intermediate glass transition-devitrifications that are invisible on the solid curve of Figure 8 are here small but discernible at a_2, b_2 on the curve of −10°C annealed wood (dashed curve) and they too have become larger and shifted to lower temperature after −5°C annealing, a_2, b_2 (as shown on the solid curve). A third very low temperature set of transitions a_3, b_3 appears in the −10°C annealed wood, but is invisible on the record of −5°C annealed wood. This is presumed to be the normal background components of the cytosol (glycolytic enzymes, salts, organic acids, etc.) which may play a role in limiting the upper temperature limits of intracellular stability to quench cooling by seeding the solution when the quenching temperature is too high. The a_3, b_3 transitions are presumed absent in the −5°C annealed material because significant homogeneous nucleation occurs during cooling at 100°C/min from −5°C and thus the dilute glass a_3 is assumed to be concentrated by that event.

represents the warming of the same tissue after annealing at −5°C followed by 100°C/min cooling to −160°C. The events a_1, b_1 have become much larger and occur approximately 40°C lower. They can be identified by their systematic shift in position and size as measured after exposure to intermediate annealing temperatures as shown on subsequent figures. Events a_2, b_2 represent the glass transition-devitrification of an intracellular component having a lower equilibrium glass transition than the constituents responsible for the large high temperature transition.

Figure 9 shows the warming of the same partially superhardy sample after annealing for 3 min at −10°C (dashed curve) followed by 100°C/min cooling to −160°C. This is compared to the warming of the tissue after annealing for 10 min at −5°C followed by 100°C/min cooling to −160°C (solid curve). Note that the events a_1, b_1 on the dashed curve, the same as the very small events a_1, b_1 of the −70°C stored material (solid curve, Fig. 8), became larger and dropped about 10°C in temperature compared to the sample immediately after storage. Since just before annealing for 3 min at −10°C, this material had been equilibrated at near −20°C, and since 3 min is not enough time to achieve equilibration, the sample was in equilibrium at between −20° and −10°C. Events a_2, b_2 on the dashed curve are identifiable as a_2, b_2 because the temperature relative to the a_1, b_1 events on the dashed curve is shifted the same number of degrees as a_2, b_2 on the solid curve are shifted relative to a_1, b_1 on the solid curve. The glass transition and devitrification events a_3, b_3 are barely visible on this record on the dashed curve. They are absent from the solid curve, probably due to intracellular nucleation during cooling from −5°C.

Figure 10 compares the same sample after annealing at −10°C for 10 min followed by cooling at 100°C/min to −160°C (dashed curve) to the same −5°C annealed run of Figures 8 and 9. Under these conditions, intracellular fluids and extracellular ice were essentially equilibrated befoe cooling in both runs. Events a_1, b_1, as expected, became larger and moved again to a lower temperature as compared to their positions when the intracellular solutions were in equilibrium with ice at <10°C (Figs. 8 and 9). Note also that events a_3, b_3 became prominent, indicating the presence of an intracellular domain whose stability is low at high intracellular water content.

Figure 11 represents a more complicated experiment. The sample is the same submaximally quench-hardy sample as used for Figures 8 to 10. The dashed curve represents warming from −160°C after annealing 10 min at −5°C, followed by cooling at 100°C/min to −30°C, annealing 17 min at −30°C, then finally cooling at 100°C/min to −160°C. The solid curve is warming after 10-min annealing at −5°C followed by cooling at 100°C/min to −160°C. Thus, the difference between the two treatments is that in the case of the dashed curve, fast cooling from −5°C

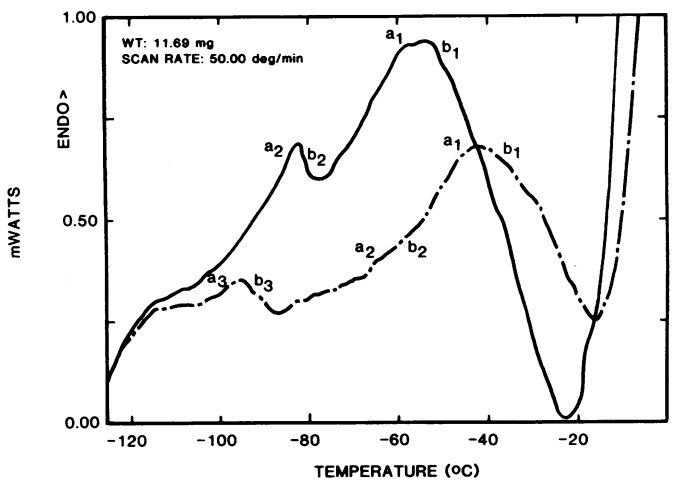

FIG. 10. Fast warming of the submaximally quench-hardy sample is shown after 10-min annealing at −5°C followed by cooling at 100°C/min (solid curve) *versus* the 50°C/min warming of the sample after 10-min annealing at −10°C followed by cooling at 100°C/min (dashed curve). This figure differs from Figure 9 in that the annealing at −10°C is more than 3 times as long; as a result, the intracellular solution that is represented by the dashed curve is much closer to equlibrium with ice at −10°C. The results are fully consistent with the patterns in Figure 9. The highest glass transition-devitrification a_1, b_1 have again moved to lower temperatures and become larger in magnitude. This is the result of increased water content due to the higher equilibrium temperature of the intracellular contents. Likewise, the intermediate glass transition-devitrification a_2, b_2 are also larger and at a lower temperature. The same holds for the lowest temperature glass transition-devitrification a_3, b_3. Note the contribution a_3, b_3 appear to make to the seeding of the intracellular medium. The glass transitions a_1 and a_2 are at or above the temperature of any events seen on cooling at 50°C/min in records of wood annealed at −10°C (Fig. 14). Thus, if this a_3 component had not been present it would be hard to rationalize either homogeneous nucleation during fast cooling or devitrification during fast warming.

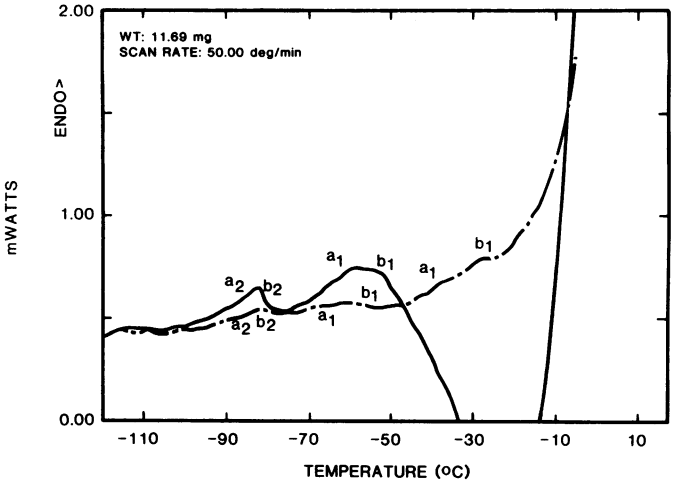

FIG. 11. This comparison of fast warming curves in the same submaximally quench-hardy samples as in Figure 8 to 10 shows the results of attempting to reestablish equilibrium in the neighborhood of the equilibrium glass transition of the major high-temperature glass-forming component. The solid curve is the 50°C/min warming of the sample after 100°C/min cooling to −160°C from 10-min annealing at −5°C. The dashed curve is the 50°C/min warming of the sample after it had been annealed 10 min at −5°C, cooled at 100°C/min to −30°C, held at that temperature for 17 min, and then cooled at the 100°C/min to −160°C. The three glass model (see "Discussion") predicts that if a solution is in equilibrium with ice at a temperature above the equilibrium glass transition point, and if it is then cooled to a point below that temperature quickly so that its composition remains essentially unchanged during cooling, it will lose water to ice until it approaches a composition whose glass transition is at that lower temperature. It will then have a composition more dilute than the equilibrium glass transition composition.

One would expect that a step cooling experiment such as the experiment shown here would yield a composition of less stability than a slow cooling to the high temperature glass transition. We would expect that the dynamics of re-equilibrating this tissue at temperatures such as −30°C would be much slower than at temperatures greater than −20°C because of the high viscosity associated with formation of an aqueous glass. These expectations are borne out by the dashed curve. Notice that some cells have apparently hardly changed their composition during the 17-min annealing. Thus, the lower temperature a_1, b_1 and a_2, b_2 match those on the −5°C curve well. Other cells have moved towards equilibrium at −30°C and thus the high temperature events at a_1, b_1 are seen as well.

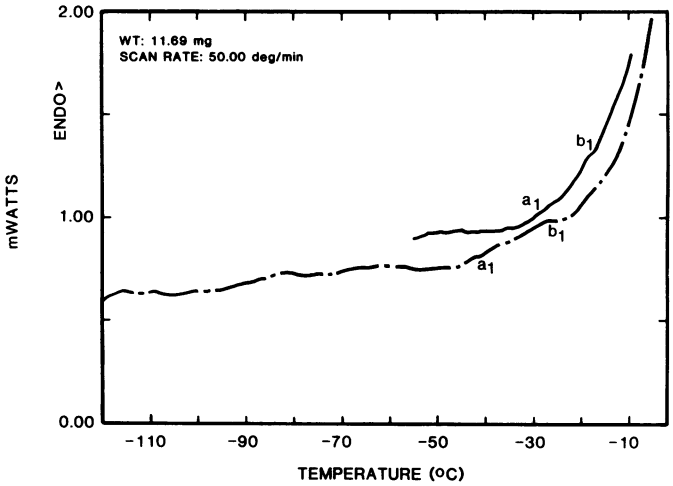

FIG. 12. Further examination of the double step cooling experiment of Figure 11. Here, the fast warming curve of Figure 8 is shown (solid curve). This material was slowly cooled to −20°C then plunged into dry ice storage for several months, warmed to −30°C for 10-min annealing to remove dry ice, then recooled at 100°C/min to −70°C before the 50°C/min warming shown by the solid curve. The dashed curve is the 50°C/min warming of the sample after annealing 10 min at −5°C, cooling at 100°C/min to −30°C, annealing there for 17 min, then cooling at 100°C/min to −160°C. As explained in DSC "Results" and Figure 11, the highest glass transition temperature that can be attained after fast cooling to a temperature below the equilibrium glass transition is the new, low annealing temperature. Since −30°C is actually about equal to the equilibrium glass transition, the fact that the glass transition-devitrification a_1, b_1, shown in the dashed curve are at a lower temperature and greater in amplitude than the corresponding transitions on the solid curve, is probably due mostly to the kinetics of cell water loss in such viscous intracellular solutions. Nevertheless, the movement of a_1, b_1 back towards the original positions and amplitudes as shown on the solid curve, but the failure to attain it during the double step cooling further strengthens the glass transition model.

was interrupted by 17 min of annealing at −30°C. These curves illustrate the complexity of the state of water in the living wood. Note that there are two sets of events labeled a_1, b_1 on the dashed curve. Also note that the low temperature events a_1, b_1 and a_2, b_2 on the dashed curve coincide on the temperature scale with a_1, b_1 and a_2, b_2 on the solid curve. This implies that some part of the intracellular medium maintained the same water content for 17 min at −30°C as it had at −5°C. Thus, the coincident peaks represent intracellular compartments that have hardly changed their composition during the annealing at −30°C. In contrast, the higher temperature events labeled a_1, b_1 on the dashed curve represent compartments that have moved toward equilibrium at −30°C. That they have not attained it is more fully illustrated by Figure 12. The dashed curve is the same as Figure 11. The solid curve is the original warming of material immediately after removal from dry ice temperature in storage (solid curve, Fig. 8). Despite the 17 min at −30°C, it is clear that even those compartments able to lose a significant amount of water have not reached as low an intracellular water content as the sample had immediately after removal from storage at −70°C.

Figure 13 shows two cooling curves of a maximally quench-hardy sample of about 10 mg. The solid curve is 50°C/min cooling of the sample after 10 min equilibration with extracellular ice at −15°C. The point a_1 corresponds to the temperature at which homogeneous nucleation events begin to appear when the material is annealed at or above −6°C. The point a_2 indicates the location of a homogeneous nucleation event that becomes prominent when the annealing temperature is at or above −8°C.

Figure 14 shows the same sample as Figure 13 but here the annealing temperature before fast cooling was −10°C (dashed curve). Integration of events a_1 and a_2 yield a total enthalpy of about 0.05 J/g.

Electron Microscopy. The electron microscope results complement the DSC results. Figure 15, a and b shows a maximally quench-hardy cell from twigs cooled at 3°C/h to −15°C, quench cooled in LN_2 at about 1,200°C/min, and then held several days at dry ice temperature before being fractured in air, also at dry ice temperature. Thus, the cell contents replicated here were in direct contact with contaminating ice for the approximately 30 min between fracturing and the time etching of the cytoplasm began. The areas labeled C are replicas of cytoplasm and show no evidence of ice formation (etching) even though the sample was held 10 min at −80°C and 10^{-9} bar. This failure to observe ice formation in the cytoplasm is in spite of the fact that, upon slow warming, the twigs from which this sample was taken displayed 100% mortality. This result is concordant with the DSC data of Figures 6 and 9 indicating that cellular contents which were in equilibrium with ice at −15°C and subsequently

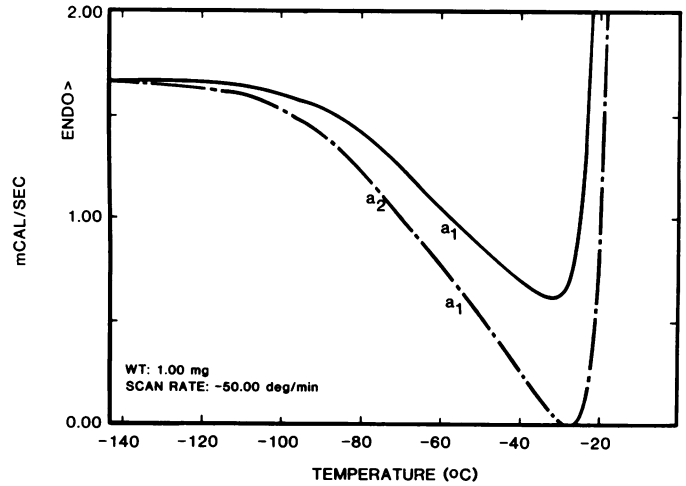

FIG. 13. Cooling record (50°C/min) of an approximately 10-mg sample of maximally quench-hardy wood annealed at −15°C for 10 min then cooled (solid curve) or annealed at −12°C for 10 min then cooled (dashed curve). 'Event' a_1 on the solid curve indicates the temperature at which freezing event is first encountered during cooling from higher annealing temperatures. This point is also labeled on the dashed curve, as is a_2, a lower temperature event also evident when cooling from higher temperatures. The most significant difference here is a generally exothermic record when comparing cooling from −12°C to cooling from −15°C. This we attribute to a larger efflux of water to extracellular ice during cooling.

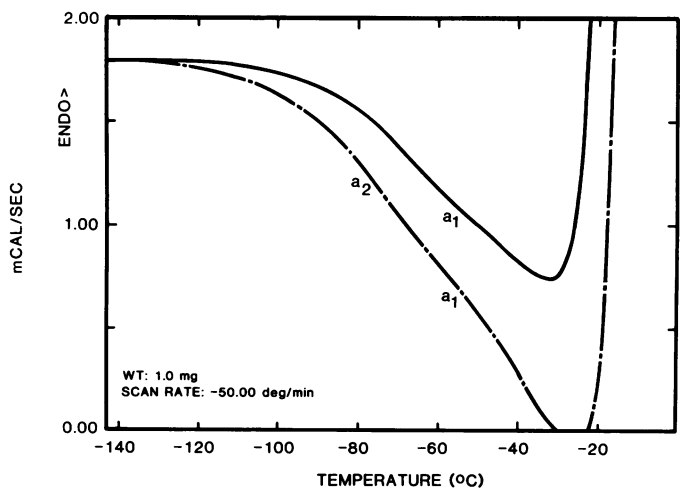

FIG. 14. Same sample as Figure 13. The solid curve is 50°C/min cooling after 10-min annealing at −15°C; the dashed curve is 50°C/min cooling after 10-min annealing at −10°C. Note that a_1 is now recognizably a deep freezing event while a_2 is questionable. If a_1 is homogeneous nucleation of a solution in equilibrium with ice at −10°C, one would predict a homogeneous nucleation temperature at or below −60°C.

quench cooled in LN_2 form unstable glasses which will devitrify during slow warming only at temperatures above −40°C.

Figure 16, a and b shows the cytoplasm and plasma membrane of a maximally quench-hardy cell from twigs cooled at 3°C/h to −15°C, cooled at approximately 1,200°C/min to −196°C, rewarmed at about 10°C/min to −27°C, held at that temperature for 12 h, and then recooled at 1°C/min to −70°C and stored. The sample was prepared by fracturing under LN_2 and etching 2 min at −90°C and 10^{-9} bar. Note the clusters of holes (arrows) indicative of ice crystal formation in the cytoplasm. This is concordant with the prediction from the DSC results (Figs. 6 and 9) that there would be formation of ice at −27°C after the quenched cells were rewarmed to and held at that temperature.

Figure 17, a and b, shows part of the contents of a maximally quench-hardy cell from twigs cooled at 3°C/h to −20°C, quench cooled in LN_2 at about 1,200°C/min, rewarmed at about 10°C/min to −27°C for 12 h, then cooled at 1°C/min to −70°C and stored. The material was prepared by fracturing under LN_2 and etched for 2 min at −90°C and 10^{-9} bar. No etching is observable either in the cytoplasm or in the interior of the chloroplast. The twigs from which this sample was taken showed 70% survival and 40% bud break/callosing upon thawing at 3°C/h. These results also agree with the DSC results in Figure 6 which indicated that when the cellular contents are quenched from an equilibrium temperature of −20°C they form stable glasses.

Figure 18 shows a submaximally quench-hardy cell (T_q = −30°C) cooled at 3°C/h to −20°C, quenched at about 1,200°C/min in LN_2, warmed to −27°C at about 10°C/min, held at that temperature for 12 h, cooled at about 1°C/min to −70°C, and stored. Samples were fractured under LN_2 and etched 2 min at −90°C and 10^{-9} bar. Note that the cytoplasm shows little evidence of etching (except perhaps in one organelle) but that the vacuole is apparently completely frozen. This implies that vacuolar contents are less stable glass formers and that their massive devitrification upon warming may be sufficient to cause cell death.

DISCUSSION

This study has led to a model of what happens to intracellular solutions in *P. balsamifera* var. *virginiana* during deep freezing in midwinter. The model asserts that there are at least three identifiable glass transitions. These are second-order phase transitions characterized by discontinuities in the second derivative of the free energy, equivalent to the heat capacity of the solution:

$$\left(\frac{\partial^2 G}{\partial T^2}\right)_P = -\left(\frac{\partial S}{\partial T}\right)_P = -Cp$$

each at a different, compositionally dependent temperature, T_g (1, 5). The direct evidence for these transitions is their appearance on Figures 5 to 12 during warming. Additional strong indirect evidence for their existence is given by freeze-etch electron microscopy and by data on mortality after quench cooling of the wood in LN_2, followed by slow warming. We shall examine the DSC evidence below and show how it leads to predictions of certain electron microscopic and mortality behavior which were also observed. Then, the calorimetric behavior of frozen aqueous PVP solutions will be compared to that of the frozen *Populus* wood. Finally, we will examine some implications of the existence of natural intracellular high temperature glass formation as a cryoprotective strategy.

Evidence for Intracellular Glass Formation. During warming through the glass transition temperature, there is a finite jump in the heat capacity of a frozen glass forming solution. The size of the power excursion recorded by a DSC scanning such a solution will be approximately linearly proportional to the rate of heating. As a result, at sufficiently slow heating rates only the largest of the glass transitions will be distinguishable from noise. This is the case in Figures 5 to 7 which show a maximally quench-hardy sample warmed at the relatively slow rate of 10°C/min. As noted in DSC "Results," the larger size and the lower temperature of occurrence of the glass transition in the run equilibrated at −20°C (a_1 on solid curve of Fig. 5) as compared to the material after cooling at 3°C/h to −70°C (a_1 on dashed curve of Fig. 5) is as expected. This is because a glass forming solution has a higher water content after equilibration at −20°C followed by rapid cooling than after slow cooling to −70°C. Also, there is no evidence of ice formation during warming, *i.e.* there is no exotherm in the material equilibrated at −20°C. These

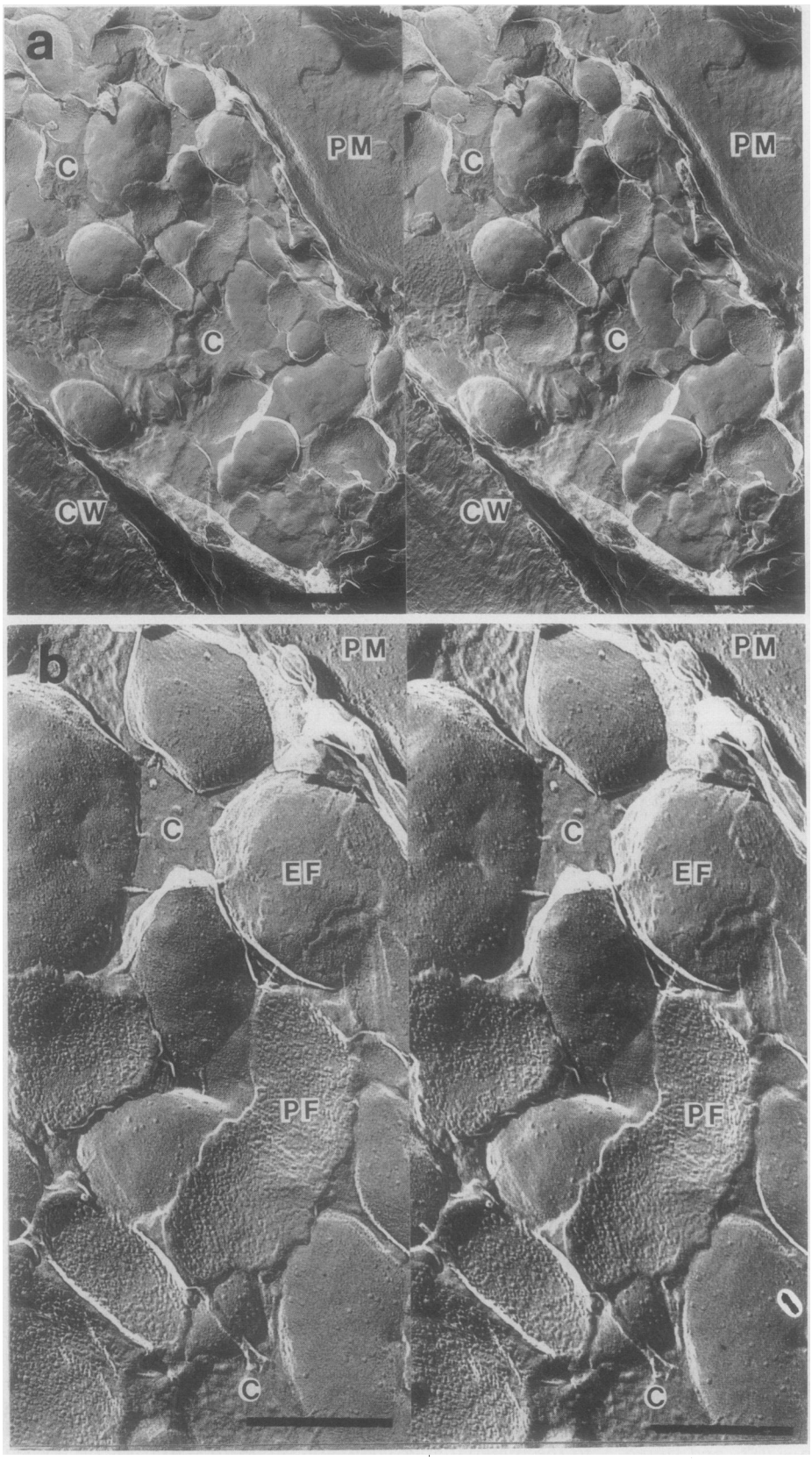

FIG. 15. a, Maximally quench-hardy *Populus* cooled at 3°C/h to −15°C, and then plunged into LN_2 (cooling 1200°C/min). The twig was subsequently fractured in air at −70°C, placed in an evacuation chamber at −110°, then etched at −80°C and 10^{-9} bar for 10 min. Note the cytoplasmic surface (C) shows no evidence of etching at this magnification. Particles on the plasma membrane (PM) are 10 to 20 nm in radius. Ice crystals, if present in significant quantity, must be considerably smaller than 10 nm. The fibrous structure in the lower right is cell wall (CW). Black bar equals 0.5 μm. × 29,000. b, An enlargement of the cell contents of the cell of (a). The E face (EF) and P-face (PF) of organelles are indicated as well as plasma membrane (PM). The cytoplasmic regions (C) show no evidence of etching even at this high magnification. Nevertheless, this cell would have died on slow warming and both DSC (Fig. 9) and electron microscope evidence (Fig. 16, a and b) show that some ice nuclei were present in the cytoplasm of this cell. Black bar equals 0.25 μm. × 88,000.

results lead to a prediction of what one might observe in the electron microscope when material is quickly cooled from −20°C, warmed rapidly to between −20° and −40°C, recooled to below −70°C, fractured, and replicated. We would predict no sign of ice formation inside the cells (Fig. 17, a and b) because, while the cell's contents are fluid at between −20° and −40°C (because this temperature range is above the glass transition when the intracellular fluid is in equilibrium with the ice at −20°C), no ice formed upon warming according to the thermal data. This is shown by the lack of a warming exotherm in material

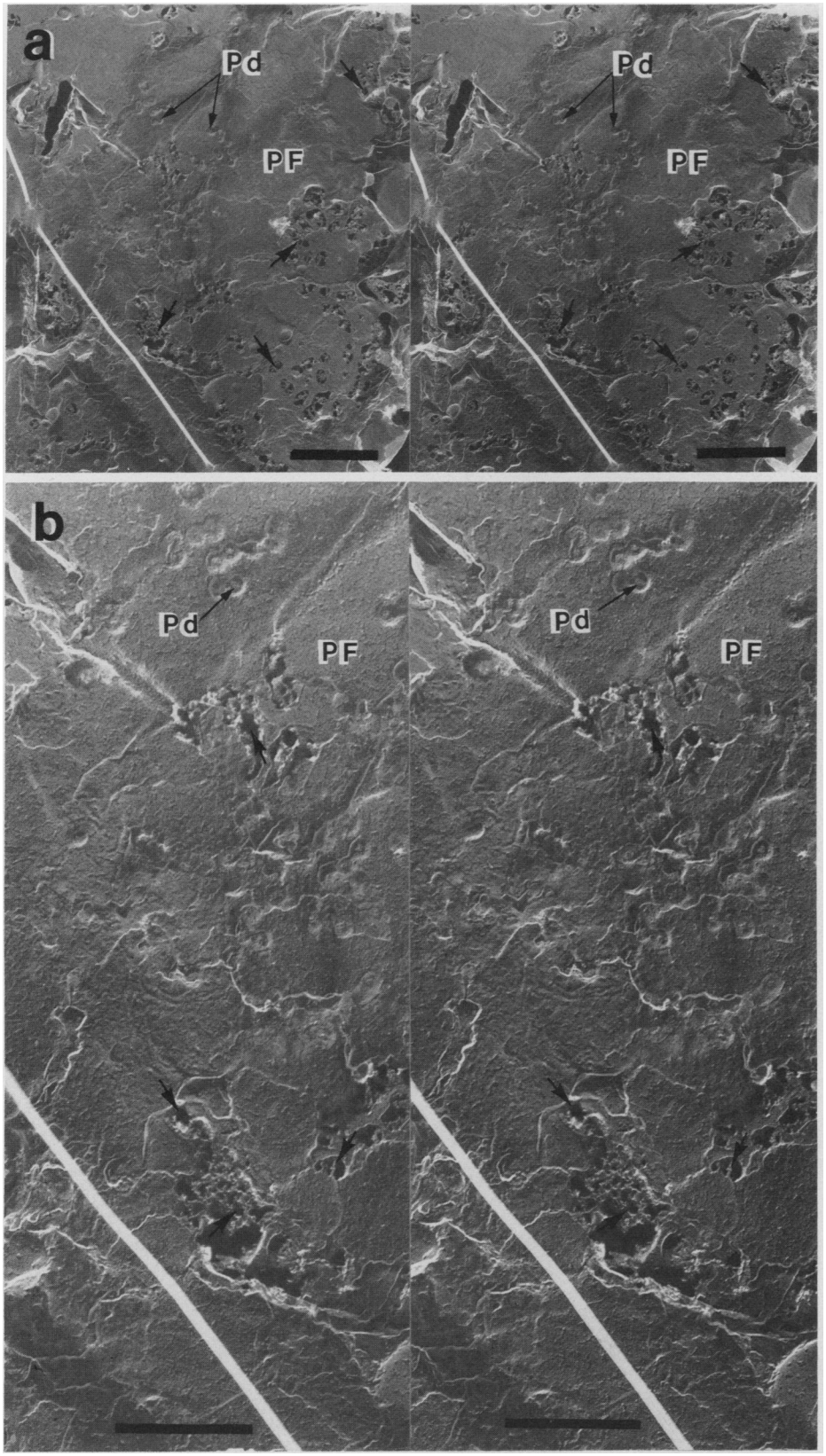

FIG. 16. a, Maximally quench-hardy *Populus* cooled at 3°C/h to −15°C, plunged into LN_2 (1200°C/min cooling), reinserted in a cooling bath at −27°C (10°C/min warming), and held for 12 h and then put in dry ice for storage (1°C/min cooling). This sample was fractured under LN_2, held at −110°C during evacuation, then etched at −90°C for 2 min. The P-face of the plasma membrane is shown (PF) as well as associated plasmadesmata (Pd). The large-headed arrows point to clearly defined clusters of holes, the remains of ice crystals of several hundred nm mean radius. Black bar equals 1.0 μm. × 13,600. b, An enlargement of Figure 16a showing P-face (PF) of plasma membrane, plasmadesmata (Pd), and clusters of holes representing intracellular ice crystals (large arrows). Black bar equals 0.5 μm. × 40,900.

first equilibrated at −20°C then quickly cooled. In this case, the electron microscope observations are even more definitive than the calorimeter measurements because the samples used in the microscope study were held at −27°C after quench cooling in LN_2 from −20°C for 12 h. Thus, ice nuclei had a much longer time to grow between −40° and −20°C than in the DSC experiment. Nevertheless, no evidence for intracellular ice formation was observed.

If intracellular ice is the lethal consequence of quench cooling, the results of Figure 5 lead to the prediction that quench cooling of maximally quench-hardy wood from −20°C and subsequent storage of the wood at −27°C for 12 h, before a second recooling

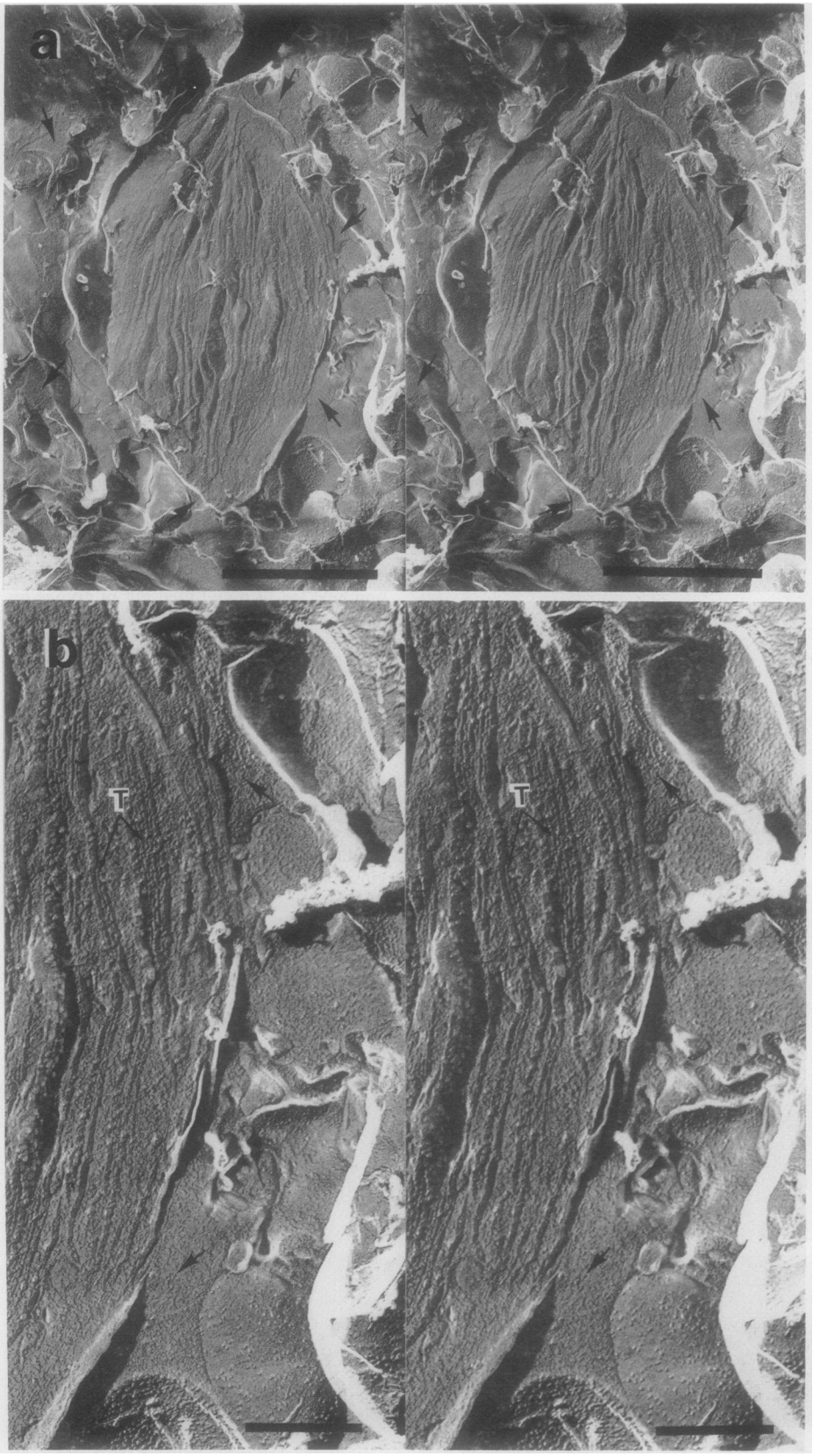

FIG. 17. a, A cross-fractured chloroplast and surrounding organelles and cytoplasm (black arrows) are shown in this maximally quench-hardy sample treated like that of Figure 16, a and b, except that initial 3°C/h cooling continued to −20°C before plunging into LN_2. Note that both the chloroplast and the surrounding cytoplasm appear completely free of evidence of etching. A sample from this tissue lived after 3°C/h warming from −70°C storage. Black bar equals 1.0 μm. × 24,000. b, Enlargement of sample illustrated in Figure 17a. The thylakoid stacks are clearly seen in an undistorted state (T) and the large headed arrows point to the smooth cytoplasm. Despite the 12 h, at −27°C and fast recooling, no observable devitrification has taken place. This corresponds well with the lack of a DSC warming exotherm in quench cooled −20°C equilibrated material (Fig. 5) and the survival of the tissue upon slow thawing. Black bar equals 0.25μm. × 72,000.

to −70°C followed by 3°C/h warming to thaw would be nonlethal. Since P = 0.49 in a sample of 24 twigs so treated (overall survival 70% *versus* control survival of 85%), this prediction was also borne out. As in the case of the material used for electron microscopic observations, the biological test ran for many hours at the potentially hazardous temperature of −27°C, allowing much more opportunity than in the 10°C/min DSC warming run for enough ice to form to kill the cells.

In Figure 6, the solid line represents the same sample as that in Figure 5 but in this scan the sample had been held 10 min at

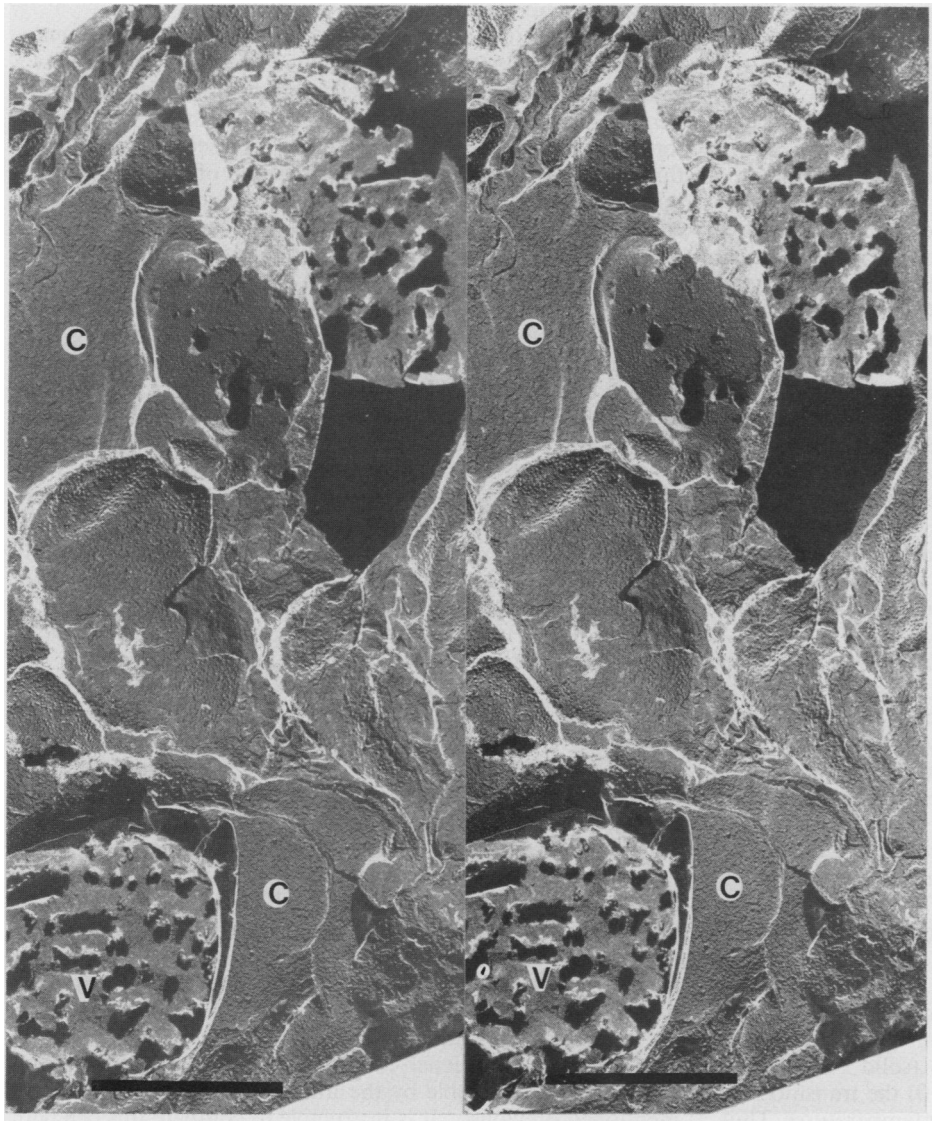

FIG. 18. A sample from a submaximally quench-hardy twig (estimated T_q = −30°C) cooled to −20°C at 3°C/h, plunged in LN_2, reinserted in a cooling bath at −27°C (10°C/min warming), held there 12 h, cooled at 1°C/min to −70°C, then stored in dry ice. The sample was fractured under LN_2, held at −110°C during chamber evacuation, then etched 2 min at −90°C and 10^{-6} torr. Note that the cytoplasmic areas labeled (C) are generally free of indications of ice whereas the vacuolar compartment (V) seems to have massively frozen. These twigs all died during a 1- to 2-week period after 3°C/h thawing from storage at −70°C. Black bar = 0.5 μm. × 50,000.

−10°C and then cooled at 100°C/min to −160°C before warming at 10°C/min. Note that the glass transition has fallen from a position in the range of −70°C to −45°C (a_1, solid curve Fig. 5) to a position in the range −100° to −60°C (a_1, solid curve Fig. 6). The broadness of these transitions is most likely due both to the poor heat transfer from and the chemical heterogeneity of the tissue. Even though the transitions are broad, the clear shifting of the glass transition to lower temperatures as well as the increase in their magnitude are what one would expect from the higher water content of the intracellular solutions in equilibrium with ice at −10°C, as opposed to those same intracellular solutions in equilibrium with ice at −20°C (*cf.* Fig. 5). The exotherm labeled b_1 on the solid curve of Figure 6 would lead to the prediction that the electron micrographs of material quench cooled from −10°C and warmed to between −50° and −25°C, and then recooled would show significant intracellular ice. It would also lead to the prediction of severe damage. Since we have not microscopically measured ice formation after quench cooling from −10°C, that prediction cannot be directly tested, but mortality is 100% for all quenching temperatures at or above −15°C. We do not display electron microscope data directly confirming the prediction from Figure 6, but present an analogous, and more powerful, measure of correlation between the calorimetry and the electron microscopy in Figure 9 and Figure 16, a and b. In Figure 9, the thermal behavior of the intracellular contents of the *Populus* is shown when a sample has been in equilibrium with ice at a temperature between −20° and −10°C then quench cooled. During subsequent warming, a small exotherm can be seen at b_1 near −30°C on the dashed curve. Assuming this to be a lethal intracellular freeze, one would predict that maximally quench-hardy *Populus* quenched from −15°C returned to −27°C, and then recooled would display evidence of ice in the intracellular medium. This is indeed seen in Figure 16, a and b. Also, the freezing is not massive but is scattered through the cytoplasm, implying that there was only a small amount of freezable water left, supporting the model further.

Figure 7 tests the prediction that the cells are able to continue to act as osmometers, excluding extracellular ice during slow cooling, even after lethal intracellular freezing had occurred. It shows the warming of the same sample from −160°C at 10°C/min after it had been annealed at −5°C to melt all pre-existing intracellular ice, cooled at 100°C/min to −20°C, annealed 10 min at that temperature, and finally cooled at 100°C/min to −160°C. In this instance, the intracellular ice formed by the devitrification event seen in Figure 6 was first melted by warming to and annealing at −5°C. The cells were allowed to reequilibrate at −20°C before quick cooling to −160°C. If the plasma mem-

branes were injured by the intracellular freeze shown in Figure 6 such that they no longer presented a barrier to ice growth into the cell, one would anticipate a warming exotherm during the 10°C/min warming after 100°C/min cooling of Figure 7. This would occur because the glassy intracellular melt in equilibrium with ice at −20°C is capable of losing water to ice at lower temperatures; otherwise there would be no difference between a warming curve of the material annealed at −20°C and quickly cooled and a warming curve of cooling at the same material after 3°C/h to −70°C (Fig. 5). The intracellular melt of the material characterized by the slow warming curve of Figure 7 (solid curve) is still in equilibrium with ice at about −20°C because during the quick cooling from −20°C no exotherm is seen (solid curve, Fig. 13). As a consequence of this reasoning, we assert that if a small amount of ice had grown through the plasma membrane during quick cooling, seeding the intracellular solution, it would have been able to grow during slow warming, causing an exotherm on the solid curve of Figure 7. This supports Levitt's (4) contention that plasma membranes of very hardy cells appear to retain semipermeability for days after thawing even following lethal freeze damage. In our own experience, hardy cells quenched in LN_2 after cooling at 3°C/h to −15°C and thawed slowly often retained semipermeability in $CaCl_2$ solutions after 10 d storage in perlite at room temperature.

Figures 8 through 12 establish that there are at least three observable glass transition-devitrification phenomena in the quench-hardy *Populus*. These figures were made during warming at 50°C/min, so, at the expense of accuracy on the temperature axis, we gained information about low energy events comparable to that obtained for the more energetic events in the 10°C/min warming records.

Note that events a_1, b_1 on the solid curve of Figure 8, representing the glass transition-devitrification in submaximally quench-hardy wood cooled at 3°C/h to −70°C, is many times smaller and at a much higher temperature than the same transitions a_1, b_1 on the dashed curve of Figure 8 seen during 50°C/min warming of wood annealed 10 min at −5°C before 100°C/min cooling. It is clear that the transitions a_1, b_1 are the same because, as the temperature at which the intracellular contents are initially in equilibrium with ice rises (solid curve Fig. 8 through the dashed curves of Figs. 9 and 10) the transitions a_1, b_1 systematically get larger and shift to lower temperatures. Thus, this glass transition occurring at the highest temperature displays behavior that is fairly typical of glass forming aqueous solutions (1, 5).

In Figures 8 to 12, the evidence for lower temperature glass transitions is also displayed. It should not be assumed that these transitions are necessarily located in anatomically separate subdivisions of the tissue. In fact, it will be argued below that the differences in behavior between the glass forming intracellular solutions and simpler binary aqueous polymer solutions are explainable because the different glass transitions are occurring within the same solutions. This multiple glass transition behavior can also be demonstrated experimentally *in vitro* in polymer-DMSO-H_2O solutions (14).

The identification of a_2, b_2 and a_3, b_3 as being equivalent between these figures is based on the constant difference in temperature between those transitions and a_1, b_1 even as the water content of the tissue decreases or increases and the position of a_1, b_1 consequently shifts. The fact that the smaller transitions move in a systematic way relative to a_1, b_1 and become larger with increased water content just as a_1, b_1 do shows that they are not noise, but represent glass transition-devitrification events. We suspect that the intermediate set a_2, b_2 may be associated with sucrose because limited HPLC data (A. G. Hirsh, R. J. Williams, unpublished data) indicates a high sucrose content in the tissue and because aqueous sucrose has an equilibrium glass transition at about −40°C (8).

Experiments involving warming of completely tender *Populus* slowly cooled to −70°C, then rapidly cooled to −160°C show a small glass transition near −70°C upon warming (data not shown here). Thus, it is reasonable to surmise that the domain which forms glass at the lowest temperature represented in Figures 8 through 12 is composed of the background of normal cytoplasmic or vacuolar soluble proteins, sugars, organic acids, salts, or all of them. In the case of tender *Populus* annealed at −22°C, cooled at 100°C/min to −160°C, and warmed at rates up to 80°C/min, there is a clear exotherm above about −40°C. Thus, the very low temperature glass forming intracellular moieties in tender *Populus* are not stable to ice growth on warming even when the intracellular solutions are in equilibrium with ice at −22°C. As a result, it is not surprising that the moieties which form glasses at the lowest temperatures in the fully quench-hardy *Populus* would nucleate the intracellular solution with ice during slow warming after quench cooling from −15°C.

Figures 8 to 12 represent results from submaximally quench-hardy *Populus* having an estimated T_q of about −30°C. This tissue was killed when cooled quickly from −20°C and slowly rewarmed. Since a small but apparently nonlethal amount of devitrification occurs during slow warming even after cooling at 3°C/h to −70°C (Fig. 8, solid curve, event b_1), it is safe to assume that a larger, lethal devitrification would have occurred in that tissue during slow warming after fast cooling from an annealing temperature of −20°C. Because the tissue was killed, one would predict that quenching of such submaximally quench-hardy material from −20°C, annealing for 12 h at −27°C and subsequent recooling would yield microscopic evidence of large intracellular ice crystals. Such ice formation is shown in Figure 18. Interestingly, most or all of the freezing seems confined to the vacuolar compartment. This implies that massive freezing of the vacuolar compartment alone is sufficient to kill the cells, and that after quench cooling from a high subzero temperature the vacuolar compartment contains vitreous solutions less resistant to devitrification during slow warming than the cytoplasmic compartment.

Comparison with Aqueous PVP. The behavior of the intracellular solutions of quench-hardy *Populus* at low temperatures seems to be explainable by the multiple glass transition model mentioned previously. It is instructive to compare this behavior to that of a well-characterized binary system of PVP-H_2O. The supplemented phase diagram for such a system is displayed in Figure 19, slightly modified from the data of MacKenzie (5).

Certain aspects of the artificial system are immediately evident. It is clear that homogeneous nucleation (the T_h curve) is only observed in solutions in which $\Delta T_m < -2$°C (as read off the T_m curve). It is also obvious that no devitrification occurs in that composition range in which homogeneous nucleation events are observed. The reason for this latter observation is straightforward. The dashed horizontal lines show the limiting concentrations achievable during homogeneous nucleation at the respective temperatures. Note that the limiting concentrations are all in a range that is stable against devitrification upon warming. These results are in sharp contrast to the DSC results for quench-hardy wood. In the wood, quick cooling from any equilibrium temperature >−10°C yields both homogeneous nucleation and, upon warming, devitrification events. In part, this is due to the fact that MacKenzie cooled and warmed at about 2°C/min, whereas the biological material was cooled at >50°C/min. Thus, the implication is that there was not enough time at such high cooling rates for both homogeneous nucleation and subsequent crystal growth to proceed to completion. It is also reasonable to postulate that the reason why homogeneous nucleation is observed in the intracellular solutions at equilibrium temperatures considerably below −2°C is that such solutions are a complex mixture of

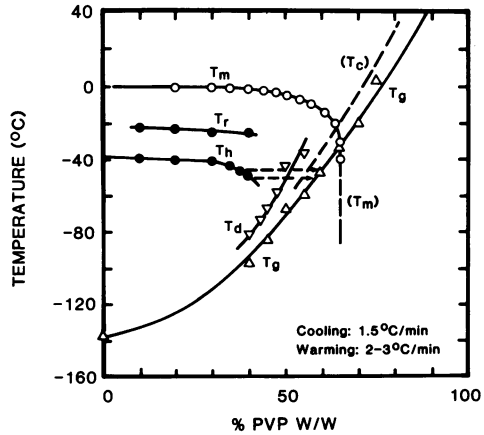

FIG. 19. Supplemented phase diagram of aqueous, 30,000 mol wt PVP according to the data of MacKenzie (5). Ordinate is percentage of PVP w/w. T_m is the equilibrium melting curve, T_g is the glass transition curve, T_h is the homogeneous nucleation curve, T_r is the ice recrystallization curve (upon warming), T_d is the devitrification curve, (T_c), hypothesized collapse temperature curve (where the glassy melt begins to flow noticeably). (T_m), an extrapolated section of the melting curve. The dotted arrows have been added to show to what composition the homogeneous nucleation of the solution will approach asymptotically at several temperatures. Note that the arrows correspond to compositions that are almost completely stable in the presence of ice on warming: thus, the lack of detectable devitrification events after homogeneous nucleation. In the composition region between 45 and 55%, where devitrification is observed, it is presumed that some homogeneous nuclei form in the temperature range between the T_d and T_g curves on both cooling and warming, but that the volume of ice formed is microscopic and undetectable with presently available instrumentation. The crossing of the T_g and T_m curves is the equilibrium glass transition. Note that there is a fairly large composition region (55–65%) between the most dilute stable glass former and the actual equilibrium glass-forming composition. Glass-forming solutions in this composition range can be cooled or warmed at any rate and no ice will form as long as heterogeneous nucleators are not present. This corresponds well with the observation that the glass forming moieties in the *Populus* are stable at compositions somewhat more dilute than the −28°C equlibrium glass forming solution.

unknown cryoprotectants and other, more usual, intracellular solutes, all of which contribute to the freezing point depression. Thus, it is not until a low enough quenching temperature is reached that the lowest temperature glass forming moiety (a_3 in Figs. 9–12) becomes stable against homogeneous nucleation and devitrification upon slow warming, conditions necessary for the tissue to survive quenching and slow warming. If we are correct, and if that moiety is composed of normal cytoplasmic components, then the upper limit of resistance to quench cooling and slow warming in any natural system forming intracellular glasses by diffusion of water to extracellular ice may be about −20°C.

The curve labeled T_r in Figure 19 traces the recrystallization of solutions frozen initially by homogeneous nucleation. Note that the temperature at which this occurred was quite high and nearly constant over a large range of initial starting concentrations. This implies that the large decrease in the temperature of occurrence of the exotherms in the quenched superhardy wood with increasing intracellular water content (higher quenching temperature) is more consistent with devitrification (*de novo* growth of ice from the melt; T_d curve in Fig. 19) than with recrystallization. Also, if the exotherms were devitrifications, one would expect that, as the glassy melt became more dilute, the amount of ice formed upon warming would increase yielding a larger exotherm. This is observed throughout the records. Nevertheless, it is important to stress that some recrystallization probably occurs as well. The enthalpy of recrystallization as a function of ice-solution interfacial free energy and the change of mean ice crystal radius in a recrystallization transition is an unsolved question in the nonequilibrium physical chemistry of water and ice (D. Rasmussen, unpublished data).

Implications of Natural Intracellular Glass Formation. Since the bulk of the intracellular solutions in maximally quench-hardy *Populus* appears to become solid below −28°C, significant additional osmotic stress would not be expected below that temperature, even at cooling rates of only a few °C/h. This is important because it is thought that many tissues of very hardy northern plants are killed by dehydration stress when intracellular solutions equilibrate with extracellular ice at below −30°C (4, 16). Intracellular glass formation might protect such tissues. That such low temperature stress in plant tissues killed below −30°C is in fact dehydration stress is suggested by experiments we conducted in which quench-hardy *Populus* was dried at −6°C in $CaCl_2$. When whole tissue water content dropped from 1.0 g/g dry weight (normal winter minimum) to 0.6 g/g dry weight no increase in mortality was seen upon subsequent reimbibition of water by the tissue. Below 0.6 g H_2O/g dry weight mortality increased rapidly with further drying and was 100% by 0.4 g H_2O/g. This is consistent with unpublished results of Siminovitch on the drought resistance of completely hardy black locust (*Robinia pseudoacacia*) bark. What it implies is that the formation of the solid intracellular glass at about −28°C prevents further water loss to extracellular ice at lower temperatures and that this is a necessary component of the cryoprotection because the *Populus* cells are not especially drought resistant. Such an interpretation contradicts the widely held idea that extreme cold hardiness is always more or less equivalent to extreme drought hardiness (4, 16).

CONCLUSIONS

In this study, we have demonstrated a novel method of natural cryoprotection: intracellular glass formation at high subzero temperatures in winter acclimated *P. balsamifera* v. *virginiana*. We have shown that the bulk of the intracellular solutions in hardened poplar trees form glasses at about −28°C during slow (less than 5°C/h) cooling. We have also demonstrated at least two additional glass forming moieties in the intracellular solutions, moieties which solidify at about −45° and −70°C during slow cooling. The proof of this three-glass model rests primarily on DSC data showing the three glass transitions. Additional proof has been supplied through a correlation between devitrification events observed in the DSC during warming scans of hardened wood after fast cooling from lethally high subzero temperatures, the minimum temperature at which very fast (1200°C/min) cooling and subsequent slow (<10°C/min) warming is lethal, and the appearance of intracellular ice in electron micrographs of quench-hardy *Populus* frozen rapidly from above −20°C at 1200°C/min.

Acknowledgments—The extensive technical difficulties involved in obtaining good freeze-etch replicas of frozen wood could not have been overcome without the expert assistance of Dr. Russell Steere and Eric Erbe of the Plant Virology Laboratory, United States Department of Agriculture-Agricultural Research Service, Beltsville, MD.

We also wish to thank Dr. William Rall and Dr. Gregory Fahy of this laboratory for their critical reading of the manuscript. Dr. Theo Solomos of the University of Maryland kindly allowed us to use his HPLC. We thank Robert H. Angell and Joseph Gray of the Potomac Garden Center for giving us access to their wild poplar grove.

LITERATURE CITED

1. ANGELL CA, JC TUCKER 1979 Heat capacity changes in glass-forming aqueous solutions and the glass transition in vitreous water. J Phys Chem 84: 268–272
2. DUBOCHET J, J LEPAULT, R FREEMAN, JA BERRIMAN, J-C HOMO 1982 Electron

microscopy of frozen water and aqueous solutions. J Microscopy 128: 219–237
3. JOHNSON JE JR Current Trends in Morphological Techniques, Vol 2, No 5. CRC Press, Boca Raton, FL, pp 131–181
4. LEVITT J 1980 *In* J. Levitt, ed, Responses of Plants to Environmental Stresses, Ed 2, Vol 1. Academic Press, New York
5. MACKENZIE AP 1977 Non-equilibrium freezing behaviour of aqueous systems. Phil Trans R Soc Lond 278: 167–189
6. MILLER KR, CS PRESCOTT, TL JACOBS, NL LASSIGNAL 1983 Artifacts associated with quick-freezing and freeze-drying. J Ultrastruct Res 82: 123–133
7. HIRSH AG 1985 The state of water and cell morphology in deeply frozen *Populus*. Ph.D. thesis. University of Maryland, College Park
8. RASMUSSEN D, B LUYET 1970 Contribution of the establishment of the temperature-concentration curves of homogeneous nucleation in solutions of some cryoprotective agents. Biodynamica 11: 33–43
9. SAKAI A 1958 Survival of plant tissue at super-low temperature. II. Low Temp Sci Ser B16: 41–53
10. SAKAI A 1960 Survival of the twigs of woody plants at −196°C. Nature 185: 393–394
11. SAKAI A, D OTSUKA 1967 Survival of plant tissue at super low temperature. V. An electron microscope study of ice in cortical cells cooled rapidly. Plant Physiol 42: 1680–1694
12. SAKAI A 1973 Characteristics of winter hardiness in extremely hardy twigs of woody plants. Plant Cell Physiol 14: 1–9
13. STEERE RL, EF ERBE 1983 Supporting freeze-etch specimens with "lexan" while dissolving biological remains in acid. Proceedings of the 41st Annual Meeting of the Electron Microscopy Society of America, San Francisco Press, Inc.
14. TAKAHASHI T, A HIRSH 1985 Calorimetric studies of the state of water in deeply frozen human monocytes. Biophys J 47: 373–380
15. TALSTAD I, H DALEN, P SCHEIE, J ROLI 1981 Patterns in quench-frozen, freeze-dried, blood proteins. Scanning Electron Microsc 2: 319–326
16. WEISER CJ 1970 Cold resistance and acclimation in woody plants. Hortscience 5: 3–10